Supporting Information

Breath Acetone Sensing Based on Single-Walled Carbon Nanotube-Titanium Dioxide Hybrids Enabled by a Custom-built Dehumidifier

Sean I. Hwang,[a] Hou-Yu Chen,[b] Courtney Fenk,[a] Michael A. Rothfuss,[c] Kara N. Bocan,[c] Nicholas G. Franconi,[c] Gregory J. Morgan,[a] David L. White,[a] Seth C. Burkert,[a] James E. Ellis,[a] Miranda L. Vinay,[a] David A. Rometo,[d] David N. Finegold,[e] Ervin Sejdic,[c] Sung Kwon Cho,[b] Alexander Star[, a, f]*

[a] Department of Chemistry, University of Pittsburgh, PA 15260, United States

[b] Department of Mechanical Engineering and Materials Science, University of Pittsburgh, PA 15261, United States

[c] Department of Electrical and Computer Engineering, University of Pittsburgh, PA 15261, United States

[d] Department of Endocrinology, University of Pittsburgh, PA 15213, United States

[e] Graduate School of Public Health, University of Pittsburgh, PA 15261, United States

[f] Department of Bioengineering, University of Pittsburgh, Pittsburgh, PA 15261, United States

*Corresponding author. Email: astar@pitt.edu

Table of Contents

Experimental Procedures

1. Chemicals and Materials

Silica gel, polypropylene film, and Mylar film were purchased from Fisher Scientific. 3 Å molecular sieve, Nafion, and calcium chloride were procured from Sigma Aldrich, and the SU-8 2075 solution and developer from Microchem.

2. Electron Microscopy

TEM images were taken using a FEI Morgagni microscope operating at an acceleration voltage of 80 keV. The SEM images were acquired using a SEM ZEISS Sigma500 VP microscope operating at an accelerating voltage of 3 kV.

3. Response Calculation

Sensor response was calculated by taking the current at the start of the purge and subtracting it from the initial current before exposure to the analyte and dividing by the initial current.

$$Response = \frac{I_{initial} - I_{purge}}{I_{initial}}$$

4. Signal to Noise Ratio and Limit of Detection Calculation

To calculate the signal to noise ratio (S/N), the sensor response to acetone was considered to be the signal. The noise was then defined as the standard deviation of the baseline current for the 30 seconds before the exposure to 0.96 ppm acetone. This variation in the baseline current was considered to be the intrinsic noise of the sensor.

$$Signal\ to\ Noise\ Ratio = \frac{Response}{\sigma}$$

The limit of detection (LOD), defined as S/N =3, was calculated by dividing the concentration of the acetone of the lowest experimentally detectable concentration of acetone, which were 0.96 ppm without the humidifier and 9.6 ppm with the humidifier, by the calculated signal to noise ratio and then multiplying by 3.

$$Limit\ of\ detection = \ 3 * \frac{0.96\ ppm}{S/N}$$

5. Energy-Dispersive X-Ray Spectroscopy

The EDX spectrum was collected using a Zeiss Sigma 500 VP FE-SEM equipped with an Oxford Microanalysis detector. Spectra was collected after focusing the beam on a homogeneous area of SWCNT@TiO_2 that had been dried onto commercially sourced copper foil from Sigma-Aldrich. The acceleration voltage used was 10 kV, and the working distance was 8.5 mm.

6. Power X-Ray Diffraction

PXRD was conducted utilizing a Bruker D8 XRD system equipped with LynxEye detector. SWCNT@TiO_2 was dried onto a glass slide for analysis. 2θ angles between 22° and 80° were scanned at 0.04° intervals with a rate of 0.4 seconds/point. The X-ray source used was Cu Kα held at 40 kV and 40 μA utilizing a 0.2 mm aperture slit width.

7. Condenser Microchannel Fabrication

To make the silicon channel mold, a silicon wafer was cleaned with a wet etch (3 parts H_2SO_4:1 part 30% H_2O_2). On the cleaned wafer, approximately 200 μm thick SU-8 2075 film was casted by spin coating the SU-8 solution at 1250 rpm. The casted film was soft baked at 65°C for 7 minutes followed by 95°C for 30 minutes. A quartz emulsion mask with 500 μm wide and up to 36 mm long channels was used to cure the film with UV (350-400 nm) radiation for 60 seconds. The Post Exposure Bake (PEB) was done at 65°C for 5 minutes followed by 95°C for additional 15 minutes. The SU-8 developer (Microchem) was used to rinse and remove the uncured portions of the film. The developed film was then hard baked at 200°C for 15 mins.

To fabricate the PDMS microchannels, the silicon wafer mold was wrapped around with aluminum foil to make a temporary dish. Solution of Sylgard 184 PDMS (10 elastomer:1 crosslinker) was poured into the mold and then placed in a vacuum desiccator to remove any air bubbles. The PDMS was cured at 150°C for 15 minutes. The PDMS microchannel was cutout using a razor blade and peeled off from the mold. The holes for the inlet and outlet tubing were made using a PDMS puncher. The PDMS microchannel was treated with plasma and then bonded to a 40x40 mm sized silicon wafer.

8. Breath Bag Compressor

The breath bag compressor was fabricated using a 18.9 L steel round pail (Grainger) with a lever lock rid. A 6.35 mm barbed hose fitting was added to side of the pail as the inlet port and a 6.35 mm PTFE female connector was added to the opposite side of the inlet port as the outlet port.

9. Breathalyzer Prototype

9.1. Electronics

The Power Management portion of the design converts either the +5 V USB power (via the mini-USB port) or the 3.7 V LiPo battery to a regulated 3.3 V for the entire device's electronics. The battery charger/controller handles recharging the LiPo battery and simultaneously powering the system when the +5 V USB connection is made.

The core of the System Control and Communication portion of the design is the CC1110 MCU. The MCU uses the I/O expander, via a 4-wire Serial Peripheral Interface (SPI) to enable each SWCNT@TiO_2 sensor individually. The MCU also writes messages to the LCD. If the +5V USB connection is made, then the MCU can communicate with a computer host via USB through the USB-to-Serial Converter (FT232).

The PWM-to-DC Converter converts the Pulse-Width Modulation (PWM) signal output from the MCU to a direct current (DC) voltage. The conversion is accomplished through a filter network situated between two op-amp buffers.

The Wheatstone Bridge Instrumentation Amplifier, Wheatstone Bridge Balance Status, CNTx Load Switching, and Wheatstone Bridge are all tightly related and interconnected. The CNTx Load Switching portion is where a specific SWCNT@TiO_2 sensor load is switched into use via the MCU programming the I/O expander. Up to 7 sensors can be multiplexed. The Wheatstone Bridge uses four resistors, two sets of two resistors connected in series between the system supply voltage and ground. The voltage between the two series resistors in each of the two legs can be balanced by the PWM-to-DC Converter. The Wheatstone Bridge Balance Status activates when the Wheatstone Bridge has been balanced via the PWM-to-DC Converter. The Wheatstone Bridge Instrumentation Amplifier amplifies a difference between the two legs of the Wheatstone Bridge.

9.2. Device Enclosure and Assembly

The prototype device housing (case) was designed in SolidWorks. The case was 3D printed in two pieces (top and bottom) using PLA filament. A separate piece was printed to hold the swappable sensor board, with a handle for insertion and removal.

After 3D printing the bottom of the case, heat-set threaded inserts (McMaster-Carr Part No. 93365A120) were inserted using a soldering iron. After soldering all components on the main PCB, the battery was connected by plugging the battery connector into the socket on the PCB. The battery was secured to the PCB with double-sided tape. Standoffs were positioned between the LCD and the circuit

board for additional support. The board was then positioned in the bottom of the 3D-printed case. The top of the case was attached with #4-40 screws (the screws insert through the standoffs and the LCD board). A 16-pin SOIC package was soldered to the swappable sensor PCB. Silicon dies were then packaged into the SOIC package, and the assembled board was attached to the 3D-printed swappable insert with epoxy.

9.3. Software

When the device is powered on, there is an initialization step in which the LCD and MCU functions and ports are set up. Following initialization, the device automatically calibrates by sweeping values of the PWM to find the balanced state of the Wheatstone bridge. The value of the Wheatstone bridge differential voltage is also stored for later comparisons, via the ADC. The calibration is performed for up to seven chemiresistors, with the calibration state stored for each sensor. The number displayed on the LCD screen while calibrating corresponds to each pad of the sensor insert.

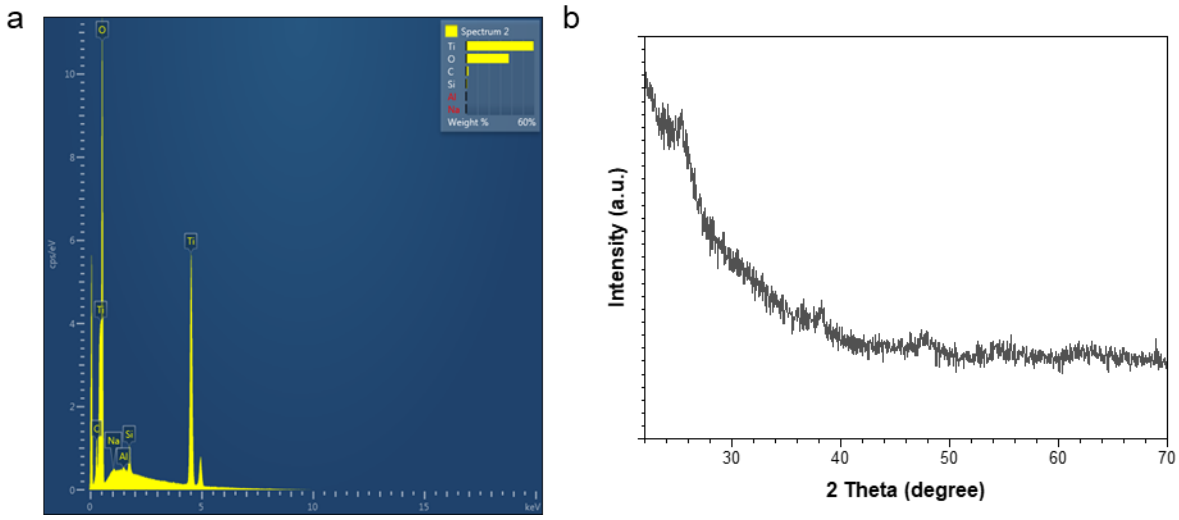

Figure S1. Characterization of TiO_2 functionalized ox-SWCNT. (a) XRD and (b) EDX of the as-synthesized material.

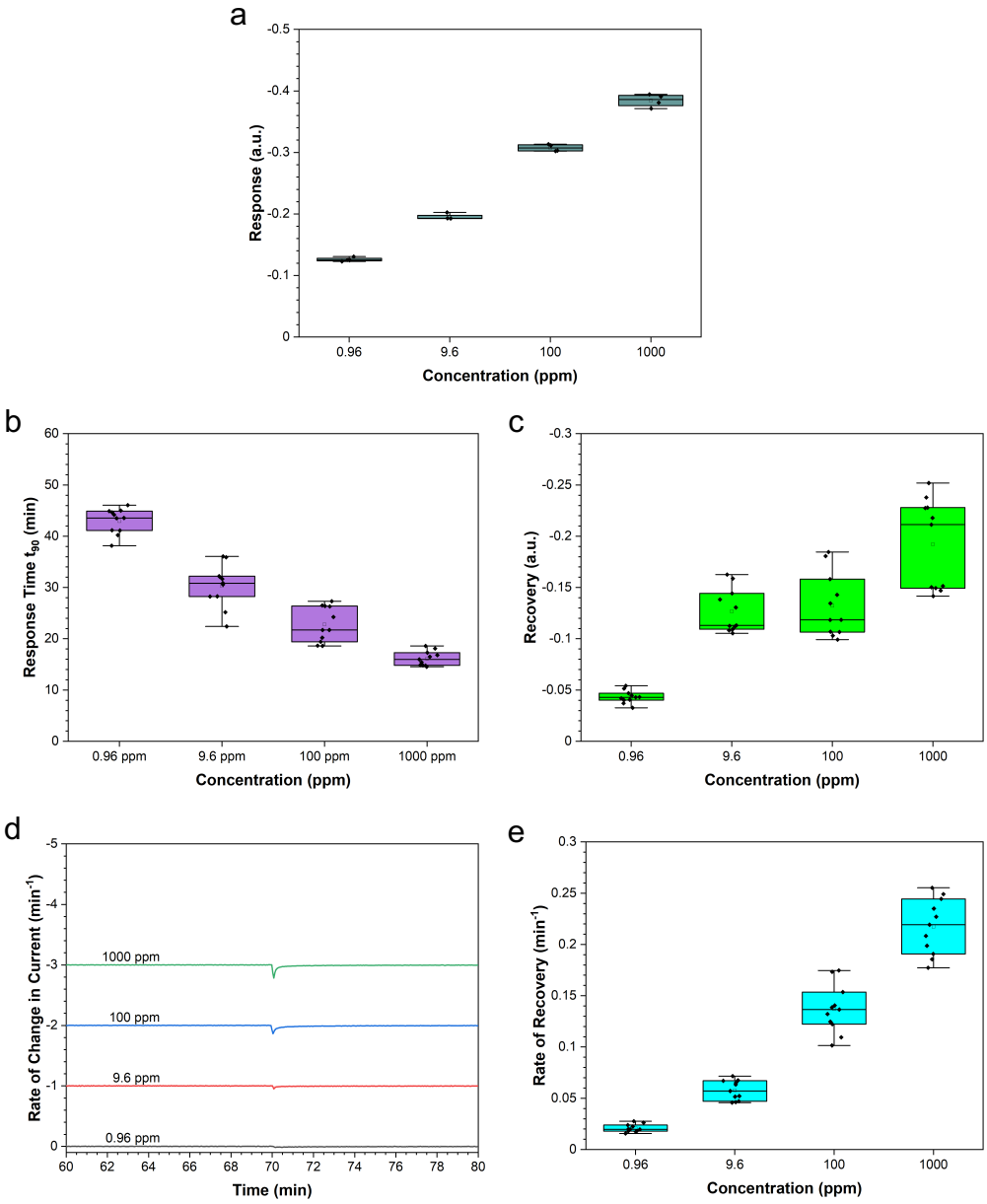

Figure S2. Acetone sensor response and recovery. (a) Acetone response of sensors with low variance. (b) Time required to reach 90% of response to 60 minutes of acetone exposure in Figure 1a. (c) Relative recovery point after 2 hours of purging with air. (d) First derivative of the sensor traces around the recovery region. (e) Maximum rate of recovery from the first derivative plot.

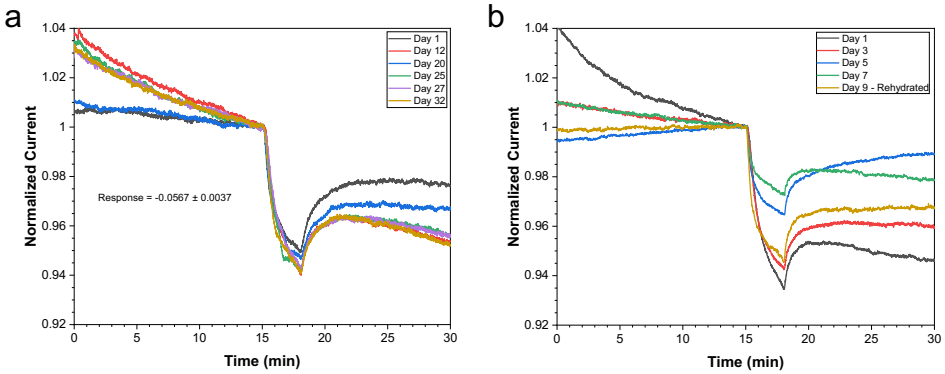

Figure S3. Response trace of a single device to 9.6 ppm of acetone. The traces were collected on multiple days. The chemiresistor was (a) hydrated with DI water for at least 10 minutes before testing or (b) stored in atmospheric conditions between runs.

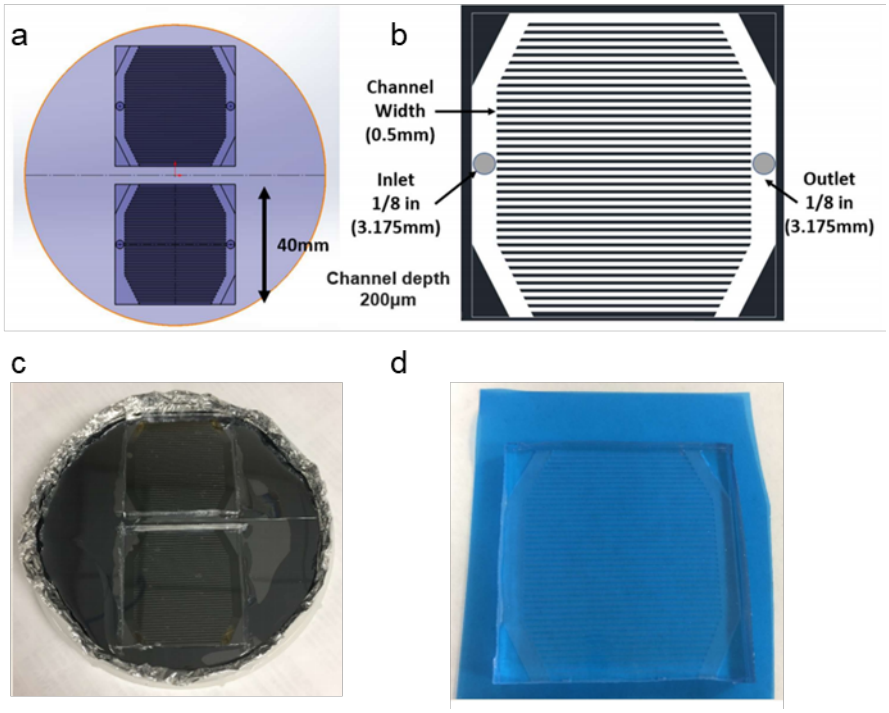

Figure S4. Condenser microchannels. (a) Diagram of the etched silicon wafer mold. (b) Diagram of the PDMS microchannel. (c) Image of the two PDMS microchannels cut out from the silicon wafer mold. (d) Image of a fabricated single PDMS microchannel.

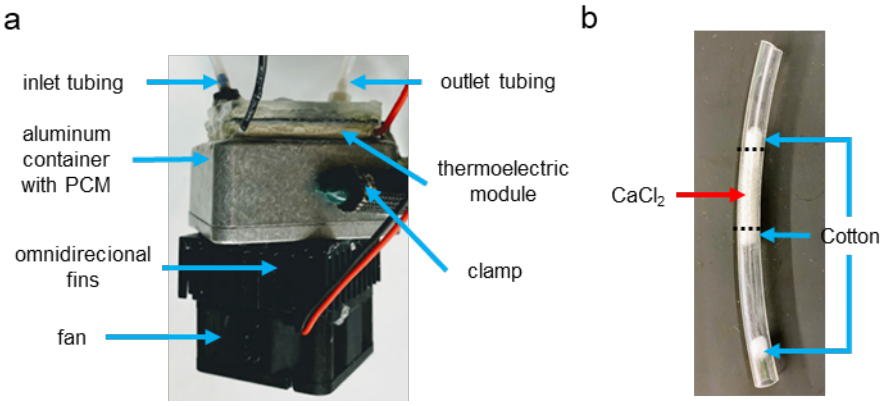

Figure S5. Dehumidifier components. (a) Image of the assembled condenser. (b) Image of desiccant plug with calcium chloride packed between two pieces of cotton. The piece of cotton at the inlet of the tubing was added to soak up any condensed water.

a

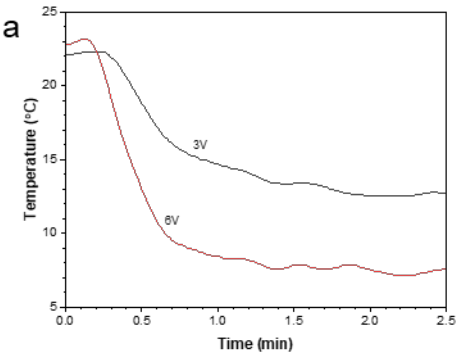

b

Voltage (V)	Temperature (°C)
2	14.1
3	12
4	10.3
5	8.2
6	7.0
7	8.1

Figure S6. Condenser voltage optimization. (a) Temperature profile of the cold side of the thermoelectric module powered at 3 V and 6 V. (b) Cold side temperature at different voltages.

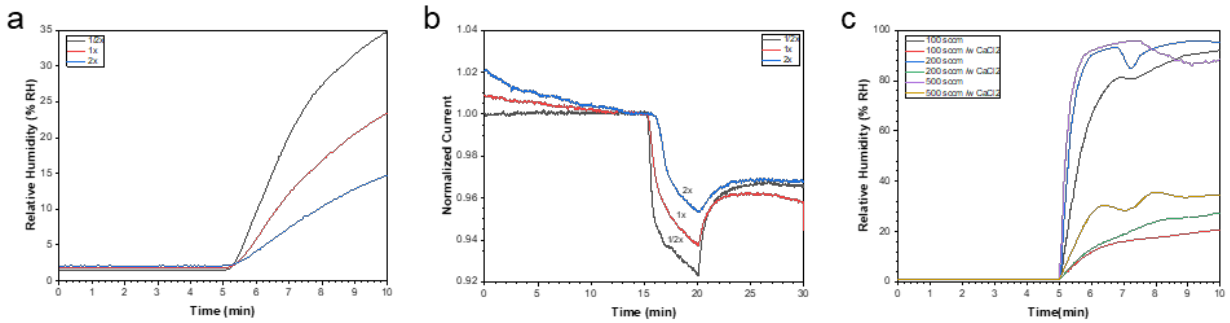

Figure S7. Desiccant plug length optimization. (a) Packing length dependency on the dehumidification efficacy of the calcium chloride plug. 1x corresponds to 25 mm of packing. (b) Sensor response dependency on the length of the calcium chloride plug. (c) Flow rate dependency on the dehumidification efficacy of the calcium chloride plug. Packing length was 25 mm.

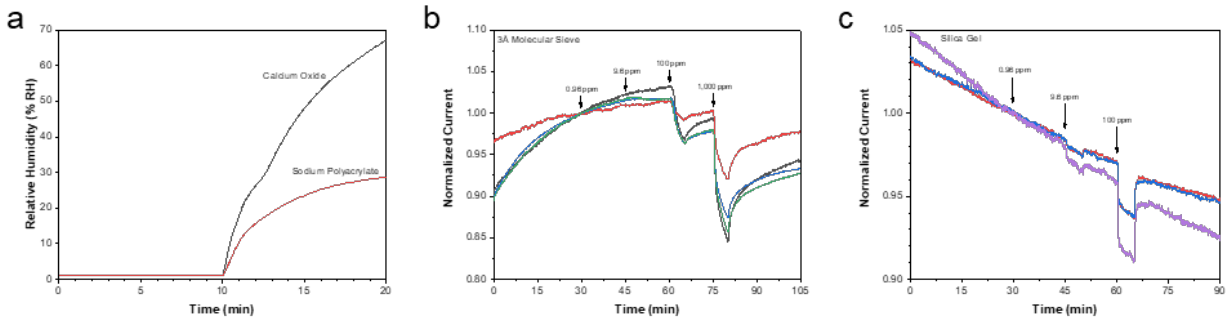

Figure S8. Desiccant comparison. (a) Dehumidification efficacy of calcium oxide and sodium polyacrylate. (b) Sensor trace measurement during exposure to gas stream containing acetone processed by 3 Å molecular sieve. (c) Sensor trace measurement during gas stream containing acetone processed by silica gel.

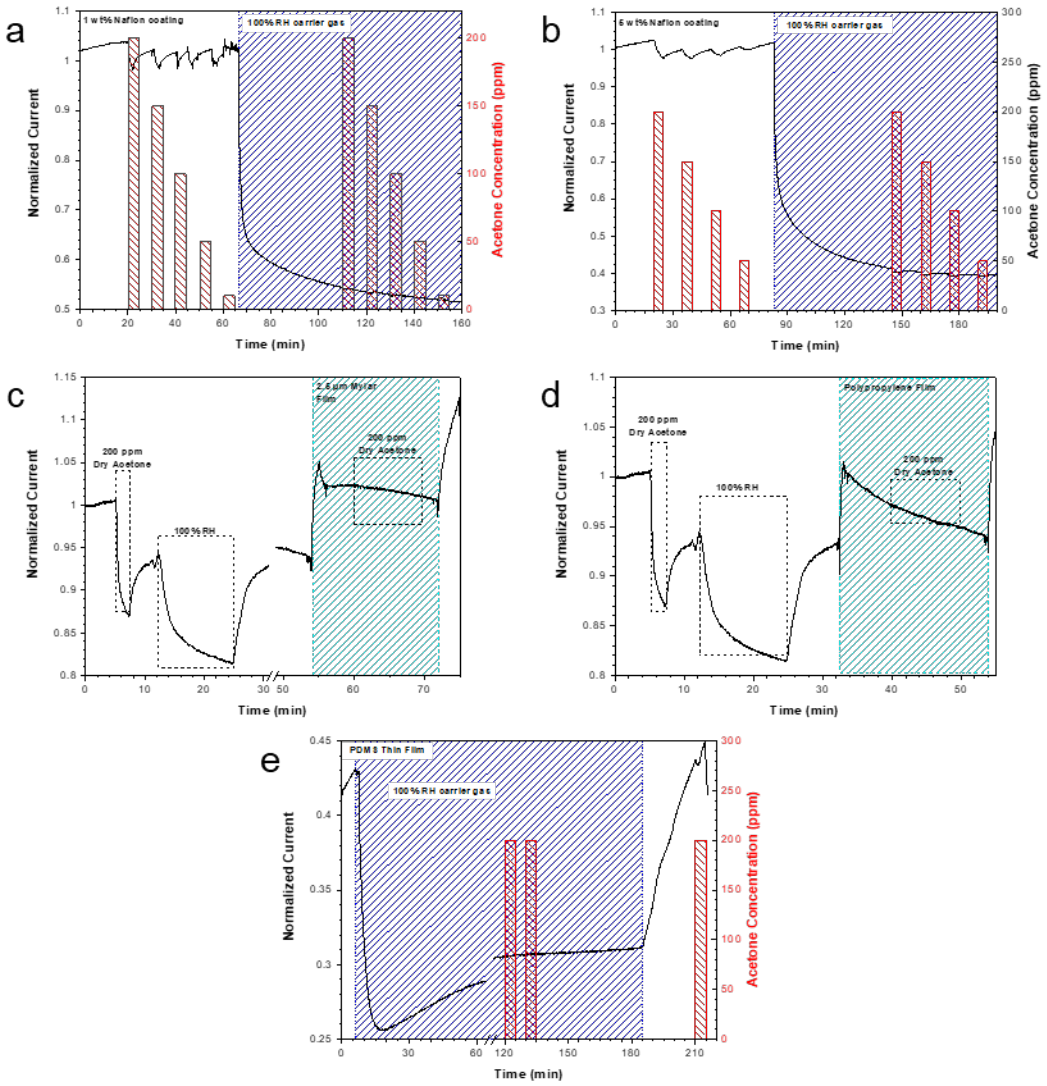

Figure S9. Thin film-based humidity reduction. (a) Sensor trace of 4 devices with 3 µL of 1 wt% Nafion/ethanol solution drop-casted and air dried on the chip. (b) Sensor trace of a device with 3 µL of 5 wt% Nafion/ethanol solution drop-casted and air dried on the chip. (c) Sensor trace of a device with PDMS spun coat on the chip at 3000 rpm for 1 minute and cured at room temperature overnight. (d) Sensor trace of a device with 6.35 µm mylar film sandwiched between the packaged sensor and the gas manifold at the 54-minute mark. (e) Sensor trace of a device with 6.35 µm polypropylene film sandwiched between the packaged sensor and the gas manifold at the 32-minute mark.

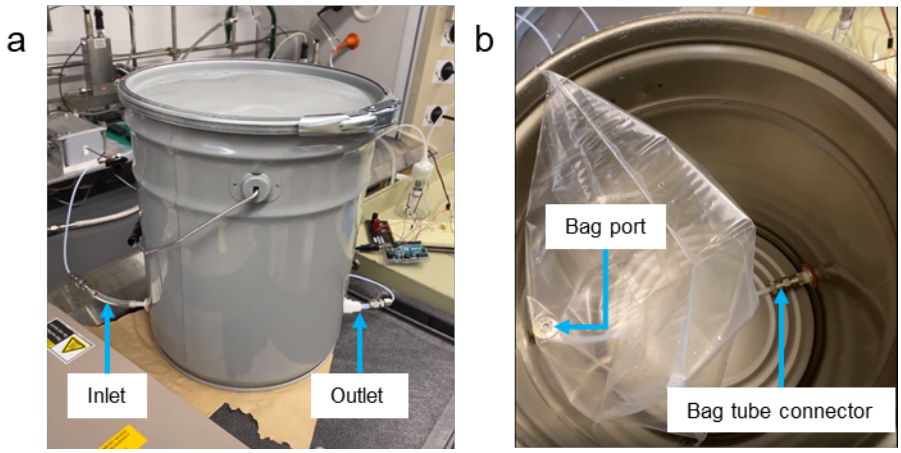

Figure S10. Breath bag compressor. (a) Image of the breath bag compressor. (b) Image of the breath bag inside the compressor.

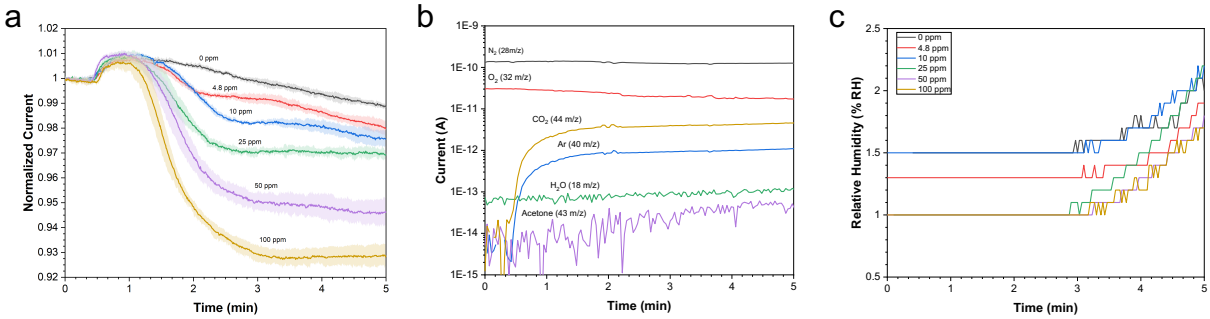

Figure S11. Tedlar breath sampling bag calibration. (a) Sensor traces of three devices exposed to the labeled concentration of acetone in the breath sampling bag. (b) Time based mass spectra of the breath bag contents containing 100 ppm of acetone after dehumidification. (c) Relative humidity of the breath sampling bag contents after drying through the dehumidifier.

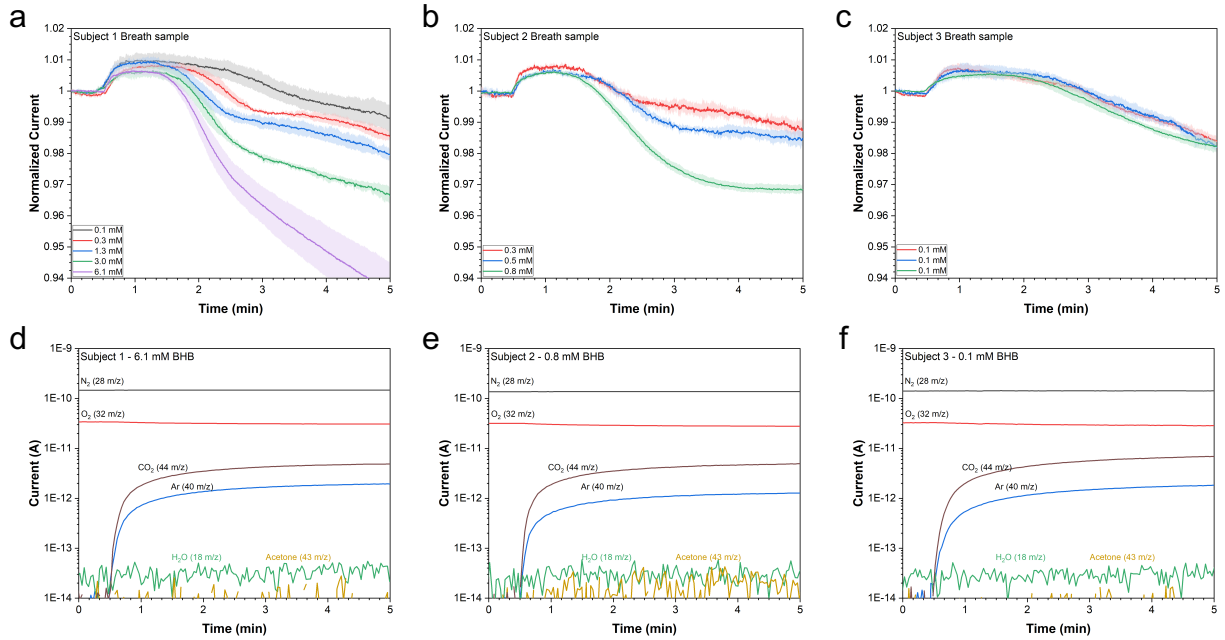

Figure S12. Analysis of breath samples from volunteers. Sensor traces of three devices exposed to breath samples from (a) subject 1, (b) subject 2, and (c) subject 3 with corresponding BHB concentrations. The shaded colored areas indicate one standard deviation. Time based mass spectra of the breath samples collected from (d) subject 1, (e) subject 2, and (f) subject 3 associated with the measured blood BHB concentrations.

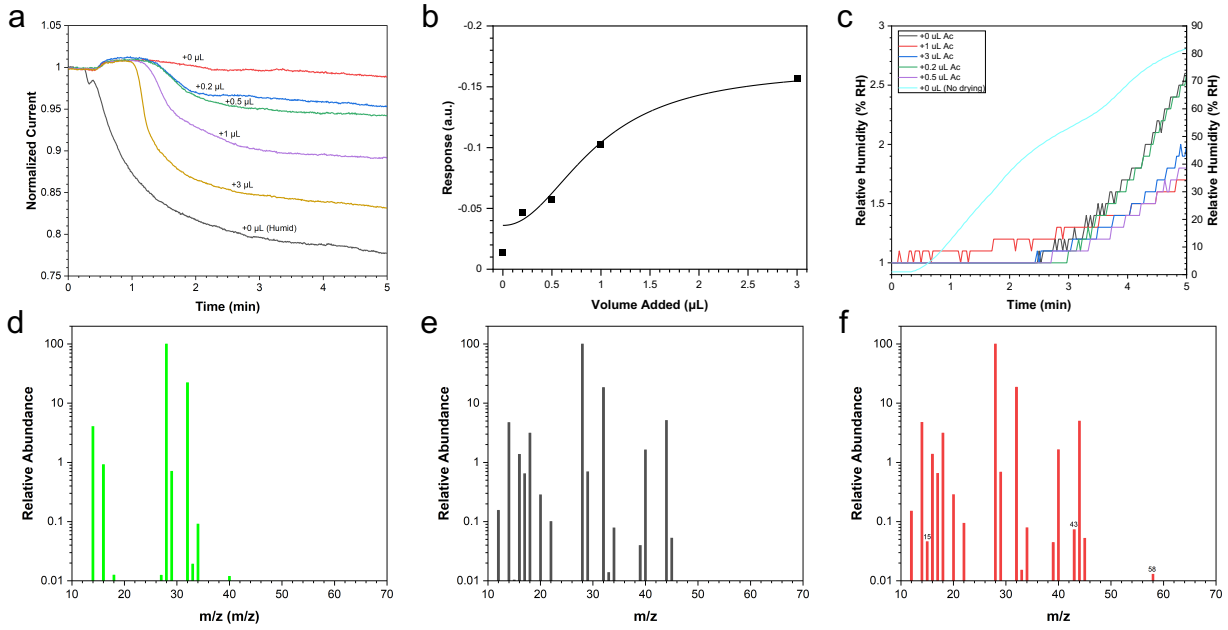

Figure S13. Acetone spiked breath samples. (a) Sensor trace of a device during exposure to acetone spiked breath samples delivered from the breath sampling bag. (b) Calibration curve of (a). (c) Relative humidity of the contents from the breath sampling bag. Mass spectra of (d) dry air, (e) breath sample, and (f) breath sample with 3 µL of acetone added.

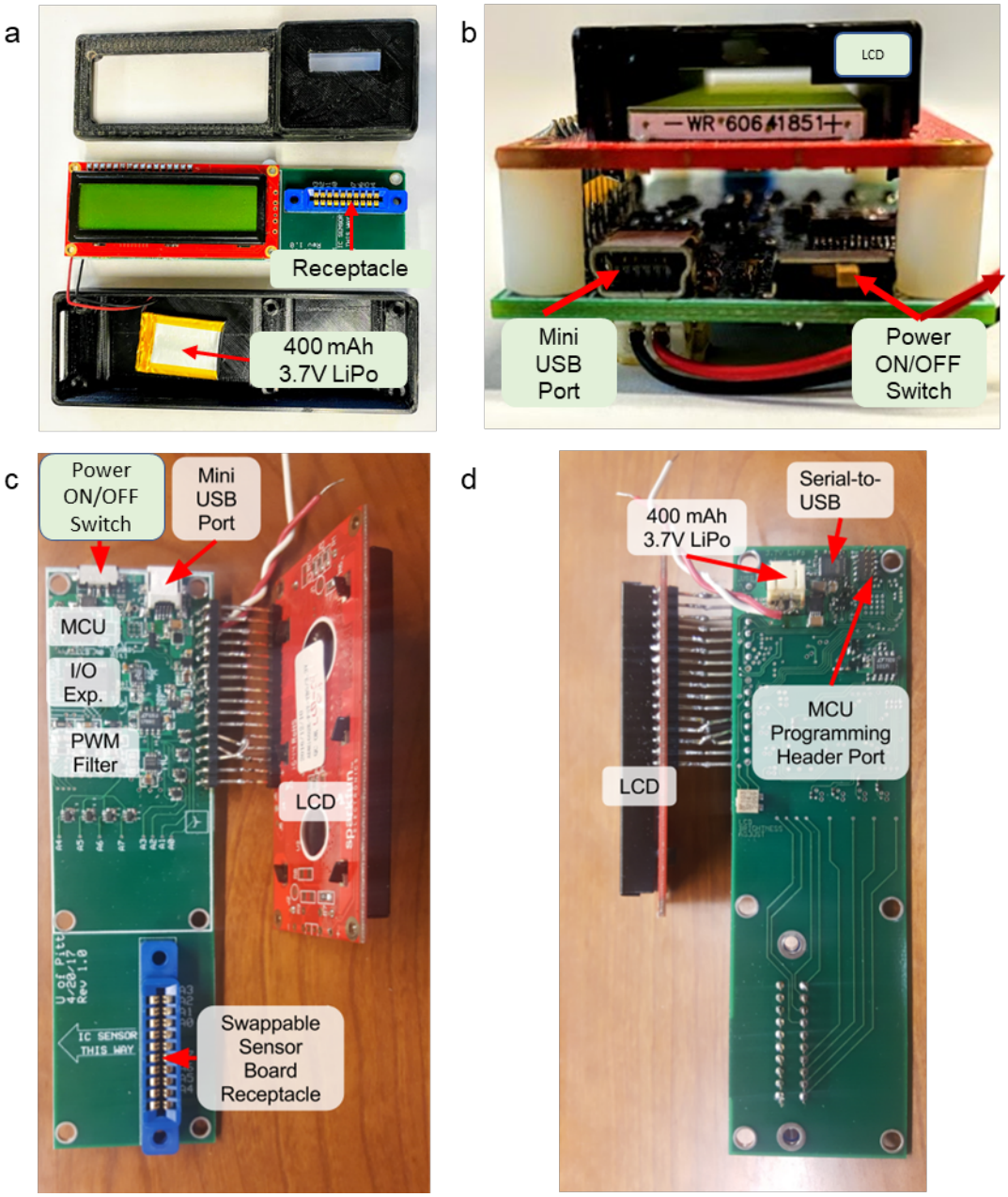

Figure S14. Prototype hardware. (a) Top down view of the prototype housing and the fully assembled circuit board. (b) Side view of the fully assembled circuit board. (c) Top down view of the circuit board below the LCD screen. (d) Bottom side view of the circuit board.

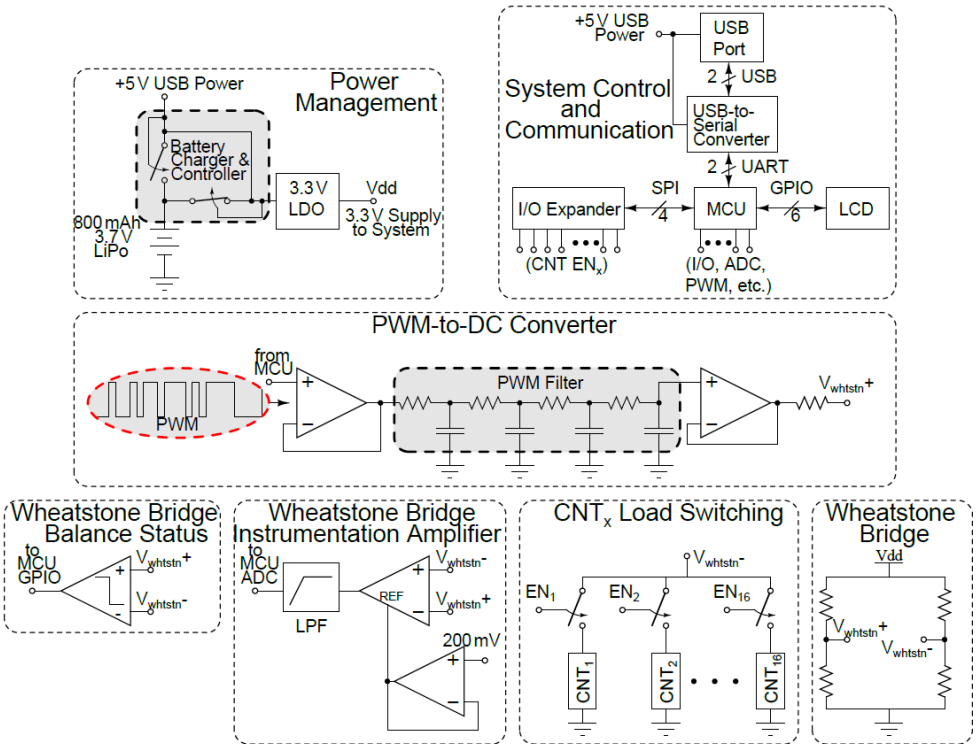

Figure S15. Prototype circuitry as described in supporting material section 6.1.

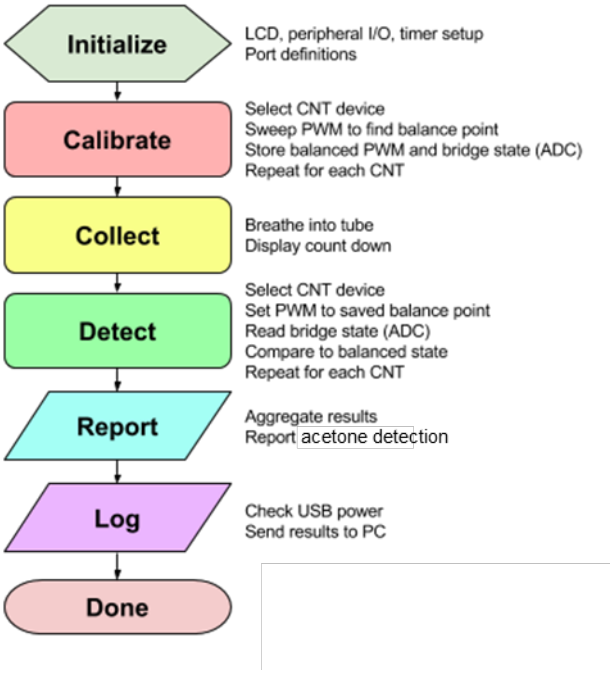

Figure S16. Prototype software diagram. The software follows the sequence of protocol for measuring breath acetone.

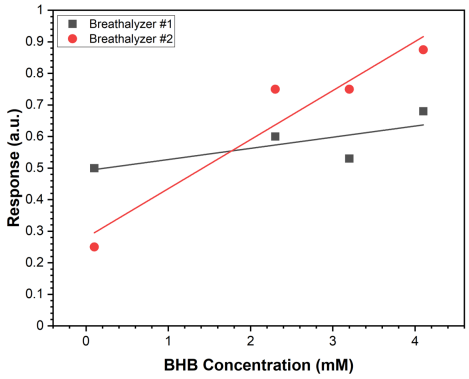

Figure S17. Breath analysis using commercially available acetone breathalyzers. The values displayed by two acetone breathalyzers after analyzing breath samples were compared to blood BHB measurements.